

# Contributions of photocatalytic/catalytic activities of $\text{TiO}_2$ and $\gamma\text{-Al}_2\text{O}_3$ in nonthermal plasma on oxidation of acetaldehyde and CO

Taizo Sano\*, Nobuaki Negishi, Emiko Sakai, Sadao Matsuzawa

*Institute for Environmental Management Technology, National Institute of Advanced Industrial Science and Technology (AIST),  
AIST Tsukuba West, 16-1 Onogawa, Tsukuba, Ibaraki 305-8569, Japan*

Received 18 August 2005; received in revised form 18 August 2005; accepted 2 October 2005  
Available online 10 November 2005

## Abstract

The effects of photocatalysis and thermocatalysis in surface discharge type plasma reactors combined with  $\text{TiO}_2$ - and  $\text{Al}_2\text{O}_3$ -based catalysts were analyzed. The photocatalytic decomposition of acetaldehyde was not observed although the  $\text{TiO}_2$  absorbed the UV light ( $300 < \lambda < 380$  nm) emitted from  $\text{N}_2$  plasma. The intensity of UV emission from plasma decreased with increasing  $\text{O}_2$  concentration. In atmospheric air, the photocatalytic decomposition rate by UV light of plasma is lower than 0.2% of the decomposition rate by the plasma itself. The coating of  $\gamma\text{-Al}_2\text{O}_3$  on the inside wall of plasma reactor improved the oxidation rate for CO by a factor of 3.5, while  $\text{TiO}_2$  improved by only a factor of 1.8, compared with the bare plasma reactor. The high activity of  $\text{Al}_2\text{O}_3$  seems to be due to the active oxygen species produced by the  $\text{O}_3$  decomposition.

© 2005 Elsevier B.V. All rights reserved.

**Keywords:** Plasma; Photocatalyst;  $\text{TiO}_2$ ; Acetaldehyde; CO; Ozone; Surface discharge

## 1. Introduction

VOCs (volatile organic compounds) are hazardous pollutants emitted from paints, solvents, preservatives, automobile exhaust gas, industrial facilities, etc. [1–5]. Recently, VOCs are also recognized as causative agents of the sick-building syndrome. In addition, emissions of VOCs can contribute to the formation of urban smog and ozone, the stratospheric ozone depletion and the greenhouse effect. Therefore, it is considered that effluent controls at the VOCs emission sources will be severe all over the world. Now, most of the small emission sources of VOCs, such as dry cleaning shop, small printing factory, and construction site using paint, take no effective environmental measures because of cost.

The conventional technique to remove VOCs is activated-carbon adsorption method, which needs to recycle and dispose the adsorbent used. The recycle of adsorbent requires energy, and the disposal will cause the next environmental problem. The alternative methods are presently being studied widely; catalytic

combustion method, nonthermal plasma method, photocatalytic method, ozone oxidation method, etc. [6–22]. Since the catalytic combustion method requires a heat source, it is highly energy-waste process when the VOCs concentration is low. Photocatalytic method using UV-illuminated titanium dioxide ( $\text{TiO}_2$ ) is expected as a safety method with low-energy consumption, since  $\text{TiO}_2$  is less toxic powder and the photocatalytic reaction proceeds in air, without any additives, and at ambient pressure [8–10]. Only UV light is required for causing degradation of VOCs. However, the performance of photocatalytic method is too low in the application for VOCs emission sources [11–14]. Alternatively, the photocatalytic method is attractive for the degradation of VOCs with lower concentration such as sick-building syndrome.

The nonthermal plasma (NTP) have been investigated by many researchers for the decomposition of fluorocarbons and VOCs, and found to have excellent performance [6,7,15–22]. Additionally, recently, it is revealed that catalysts in NTP improve the specific energy efficiency and reduce byproduct formation in the VOCs degradation [6,18–22]. In this plasma-enhanced catalyst (PEC) method, many kinds of heterogeneous catalyst, such as  $\text{BaTiO}_3$ ,  $\text{Al}_2\text{O}_3$ ,  $\text{SiO}_2$ ,  $\text{TiO}_2$ ,  $\text{MnO}_2$  and their derivatives, were evaluated. Among them,  $\text{TiO}_2$  often revealed

\* Corresponding author. Tel.: +81 29 861 8166; fax: +81 29 861 8258.  
E-mail address: [sano-t@aist.go.jp](mailto:sano-t@aist.go.jp) (T. Sano).

the higher enhancement effect on the energy efficiency. Lee et al. reported that the decomposition of benzene by using a discharge plasma-photocatalyst hybrid system using dielectric barrier discharge (DBD) plasma [18]. They described that the photocatalytic reaction by  $\text{TiO}_2$  increases the benzene conversion and the  $\text{CO}_2$  selectivity. Li et al. reported that a combination of dc streamer corona plasma and  $\text{TiO}_2$  pellet improved the toluene decomposition [19]. In these reports, the emission of UV light was confirmed but the UV intensities were not analyzed. Additionally, net photocatalytic reaction rates were not evaluated. Ogata et al. reported that the removal rate of fluorocarbons in Ar atmosphere increased when the plasma reactor was filled with  $\text{TiO}_2$  pellets as a catalyst [21]. Because significant UV emission and temperature increase were not observed during the plasma operation, they concluded that the catalytic effect seemed to be derived from the direct activation of the  $\text{TiO}_2$  surface by the plasma discharge. Thus, photocatalytic effects of  $\text{TiO}_2$  in NTP were not well understood. If the photocatalytic effects can improve the specific energy efficiency for the decomposition of VOCs by NTP, the contribution and the theoretical limitation of photocatalytic effects should be discussed. For the purpose, since UV absorption by  $\text{TiO}_2$  is essential for photocatalytic reactions, the UV intensity emitted from plasma discharge should be analyzed.

In the present paper, we assembled three types of surface discharge plasma reactors equipped with oxide catalysts, and evaluated the contributions of photocatalytic and catalytic effects on the decomposition of VOCs. The intensity of UV emission from plasma was analyzed, and the photocatalytic oxidation rate for acetaldehyde was evaluated. The roles of catalysts, deposited metals, ozone, and heat were discussed using CO oxidation reaction.

## 2. Experimental

### 2.1. Preparation of catalysts

Anatase type of  $\text{TiO}_2$  (Ishihara Co.: ST-01 and Degussa: P25) and  $\gamma\text{-Al}_2\text{O}_3$  (Sumitomo Chemical Co.: TA200I) were used.

The surface areas of ST-01, P25 and TA200I were 300, 50 and  $200\text{ m}^2/\text{g}$ , respectively. Since  $\gamma\text{-Al}_2\text{O}_3$  has no photocatalytic activity while it has enough catalytic activities, the effect of  $\gamma\text{-Al}_2\text{O}_3$  in plasma was compared with that of  $\text{TiO}_2$ . Pt-deposited  $\text{TiO}_2$  ( $\text{Pt-TiO}_2$ ) and Pt-deposited  $\gamma\text{-Al}_2\text{O}_3$  ( $\text{Pt-Al}_2\text{O}_3$ ) were also used.  $\text{Pt-TiO}_2$  was prepared by photodeposition method with P25 and  $\text{H}_2\text{PtCl}_6$  as precursors [23].  $\text{Pt-Al}_2\text{O}_3$  was prepared by chemical reduction method with  $\text{H}_2\text{PtCl}_6$  and  $\text{NaBH}_4$ . The amounts of Pt deposited were 1.0 wt.% against  $\text{TiO}_2$  and  $\text{Al}_2\text{O}_3$ . These catalysts were used without further heat-treatment or  $\text{H}_2$ -reduction.

The catalysts were coated on the reactor walls by the following procedure. A small portion of the catalyst powder was dispersed into distilled water (20 mg-cat/ml-water), and the suspension was painted on the reactor wall while sending a warm current of air to fix the catalyst, and finally the reactor was dried at  $110^\circ\text{C}$  for 12 h. The coated lengths were same as the ground electrode described later.

### 2.2. Plasma system

The configuration of the basic reactor that generates surface discharge plasma is illustrated in Fig. 1a. A quartz tube (length 180 mm, outer diameter 12 mm, inner diameter 9 mm) was used as the dielectric barrier that played a role of the reactor. A spiral stainless steel wire with a 0.4 mm diameter was set in contact with the inner wall of the barrier tube (15 turns in 100 mm). A copper foil was wrapped on the outside of barrier tube as ground electrode (100 mm length). A high-voltage ac was applied across the electrodes using a 24 kHz neon transformer (S-light Co. Ltd.: model alpha-NEON M-5). The input power (plug-in power) was measured with a digital power meter (Yokogawa Analytical Systems: model WT210). The surface temperatures of the plasma reactor were analyzed by an infrared thermography (Nippon Avionics Co.: TVS-700).

Fig. 1b shows the double tube photocatalytic reactor, where the UV light emitted from plasma was irradiated to the photocatalyst existing out of plasma region. The three windows (6 mm  $\times$  90 mm) were made on the ground electrode, through

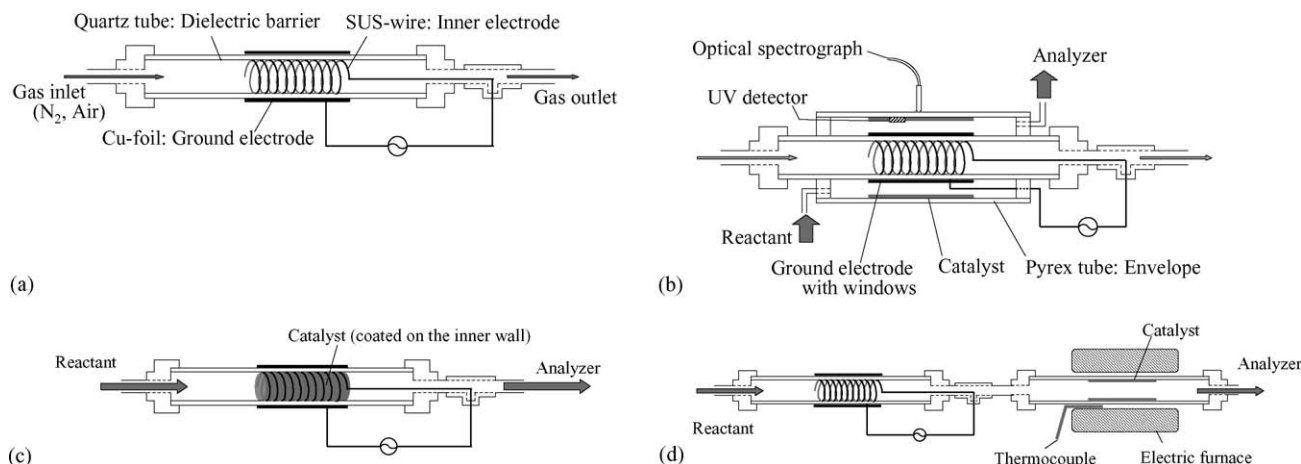


Fig. 1. Schematic illustrations of plasma reactors: (a) basic configuration, (b) double tube photocatalytic reactor, (c) plasma enhanced catalytic reactor, and (d) combined reactors.

which the UV light passed. Emission spectra from plasma discharge were measured with an optical spectrograph (Eagle Engineering Co.: LEO/CDI 200–800). TiO<sub>2</sub> powder (P25, 36 mg) was coated on the inner wall of the envelope (60 cm<sup>2</sup>) and any catalyst was not coated in the barrier tube. In this case, the effect of photocatalyst would be emphasized since the reactant gas did not contact with plasma. The reactant gas (100 ppm of acetaldehyde diluted in the air) was passed through the space between the inner tube and the envelope at the flow rate of 100 cm<sup>3</sup>/min, and the concentration of acetaldehyde in the effluent was analyzed by a gas chromatograph with FID detector (Shimadzu: GC-14B).

In the analyses of the effects of catalyst in plasma, the catalyst was coated on the inner wall of the barrier tube together with the inner electrode (Fig. 1c). The amount of catalyst was 50 mg. To remove organic impurities on the catalyst surface, plasma was generated at 5 W while clean air was passed through the reactor until the evolution of CO<sub>2</sub> stopped. The reactant gas (800 ppm of CO diluted in Ar/O<sub>2</sub> stream) was passed through the barrier tube at a flow rate of 100 cm<sup>3</sup>/min. The concentration of CO and CO<sub>2</sub> were analyzed by Fourier transform infrared spectroscopy (FT-IR, Nicolet: Magna650) with a multireflection gas cell (path length 2.4 m). The partial pressures of gases were calculated from the absorbance areas, which were calibrated with standard gases. The concentration of evolved O<sub>3</sub> was analyzed by an ozone analyzer (Ebara Co.: HARE model 620).

Contributions of thermal catalysis in the presence of O<sub>3</sub> were evaluated with the combined reactors shown in Fig. 1d. The reactant gas was same as Fig. 1c. O<sub>3</sub> was formed in the plasma reactor, and was passed through the catalytic reactor, whose temperature was controlled by a thermocouple and an electric furnace. The dimension of catalytic reactor tube was same as the barrier tube.

### 3. Results and discussion

#### 3.1. Photocatalytic decomposition rate by UV light originated with plasma

The photocatalytic decomposition of acetaldehyde (AcH) by UV radiation from surface discharge plasma was analyzed with the setup (b) in Fig. 1. N<sub>2</sub> gas was passed through the barrier tube, and then high voltage was applied to the electrodes. The input power was controlled to be 5 W. Fig. 2 shows the UV–vis emission spectra observed from the outside of envelope tube. The light emissions with the wavelengths between 290 and 400 nm were observed without TiO<sub>2</sub> coating. This UV-emission range lies within the absorption range of TiO<sub>2</sub>. When the envelope with TiO<sub>2</sub> coating was used, the UV light was not detected. This indicates the UV light from plasma was absorbed by TiO<sub>2</sub>. Since TiO<sub>2</sub> absorbing UV light generally degrades AcH as Eq. (1) [24], the TiO<sub>2</sub> coated in the envelope can also degrade AcH photocatalytically apart from the problem of its efficiency

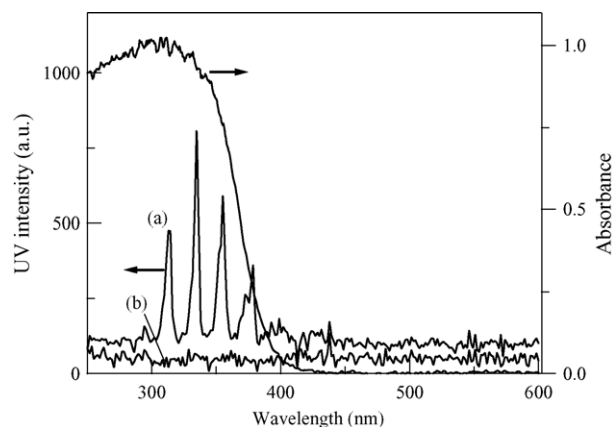
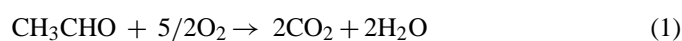


Fig. 2. UV–vis emission spectra of surface discharge plasma observed from the outside of envelope without catalyst (a) and with TiO<sub>2</sub> (b), and the diffuse reflectance spectrum of TiO<sub>2</sub>. Air was passed through the barrier tube at a flow rate of 100 cm<sup>3</sup>/min. The input power was 8 W.

However, the photocatalytic degradation of AcH by TiO<sub>2</sub> was not observed when 100 ppm of AcH gas was introduced to the reaction space between the barrier tube and the envelope. Fig. 3a shows the relation between the AcH conversion and the input power. AcH conversion was defined as follows:

$$\text{AcH conversion} = \left( 1 - \frac{\text{AcH concentration at the reactor exit}}{\text{supply concentration of AcH}} \right) \times 100 \quad (2)$$

When the input power was 0–3 W, the AcH conversions were zero. By increasing supplied voltage, the AcH conversions were increased. The increases in AcH conversions are due to the plasma and ozone generated at the ground electrode side (Fig. 3b). It seemed that parts of the edges of windows opened on the ground electrode acted as discharge electrodes. However, plasma was mainly generated in the inner electrode side since the concentration of ozone formed on the ground electrode side was much lower than that possibly formed in the inner electrode side. Therefore, it is more suitable to use the ground electrode side for evaluating photocatalytic activity. The AcH conversions with the TiO<sub>2</sub> coating were identical to that without catalyst at the input power range analyzed, and no enhancement effect was observed. This result suggests that the UV intensity of plasma is quite weak to decompose 100 ppm-level of AcH photocatalytically.

When UV light (70 μW/cm<sup>2</sup>) of black lamp bulb was irradiated to the TiO<sub>2</sub> from the outside of the envelope, 43% of supplied AcH was decomposed. Since the wavelengths of UV light irradiated were longer than 300 nm, O<sub>3</sub> was not produced. Also the temperature of the photocatalyst was similar to the room temperature. Therefore, the decomposition of AcH was due to only the photocatalytic reaction. The quantum efficiency (incident photon-to-reaction efficiency) was estimated to 28%. In this case, the total UV energy irradiated to TiO<sub>2</sub> was only 4 mW. Considering the result of Fig. 3a, the UV intensities derived from plasma with 3–8 W is estimated to be much smaller than 4 mW.

The intensity of UV light emitted from the surface discharge plasma was measured by GaN type UV sensor (Fuji Xerox Co.:

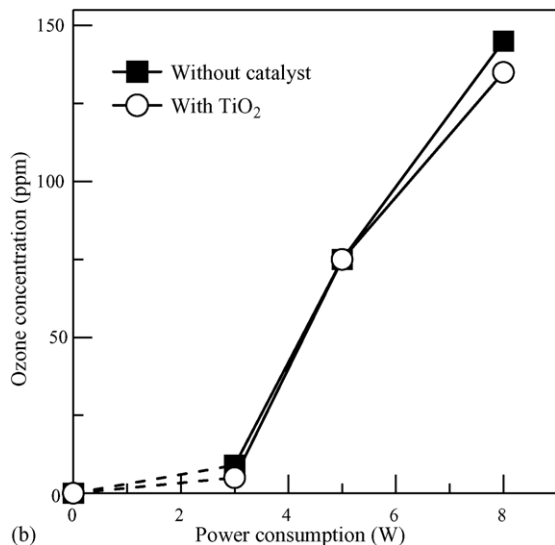
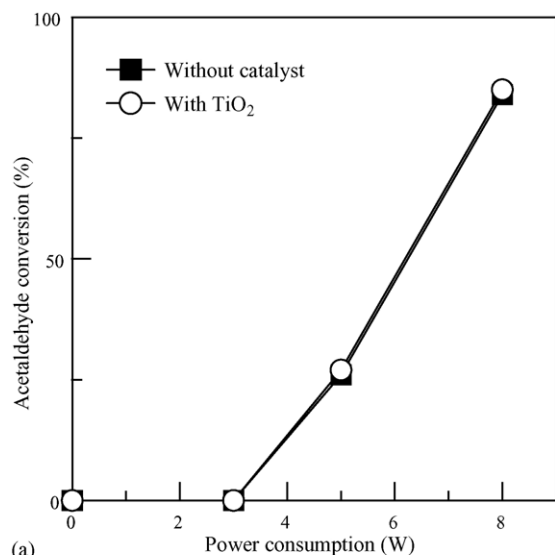


Fig. 3. Relation between the input power and AcH conversion (a), and O<sub>3</sub> concentration (b), obtained with the double tube photocatalytic reactor. The filled squares (■) indicate the values for the experiment without catalyst, and the open circles (○) indicate the values with TiO<sub>2</sub> (P25) coated in the envelope.

UV care mate Pro) placed inside of the envelope (Fig. 1b), and was shown in Fig. 4. The diameter of GaN detector was 1.5 mm. The UV intensities were analyzed while controlling the input power and the O<sub>2</sub> concentration in the gas current that was passed through the barrier tube. The total UV intensity was calculated by considering the shapes of the reactor and the window of ground electrode. UV emission was not detected below 2 W and the UV intensity increased with the input power above ca. 3 W. The UV intensity was decreased by increasing the O<sub>2</sub> concentration. This suggests that oxygen molecules act as quenching agent for N<sub>2</sub> excitation state. The total UV intensity in the atmospheric condition (O<sub>2</sub> 20%) was only 0.15 mW (ca. 2.5 μW/cm<sup>2</sup> on an average) at the input power of 5 W. The photocatalytic reaction rate at the UV irradiation of 0.15 mW is estimated to be 3 × 10<sup>-2</sup> μmol/min, assuming the quantum efficiency is 100%. On the other hand, the energy efficiencies of plasma for VOCs

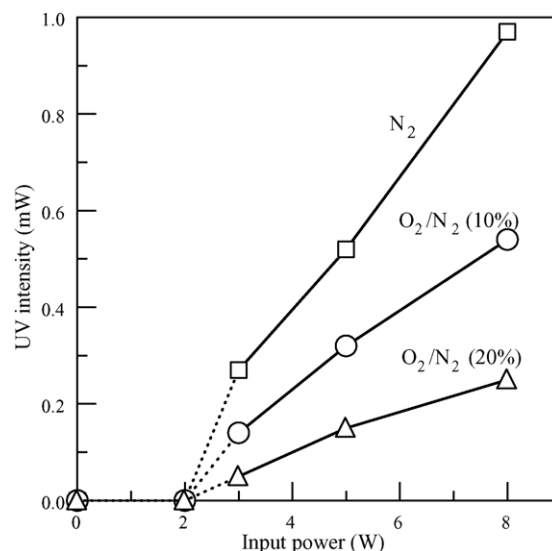


Fig. 4. Intensities of UV emission from surface discharge plasma. The total flow rate was 100 cm<sup>3</sup>/min.

decomposition were quite high. The energies to decompose benzene and fluorocarbons are 1 × 10<sup>7</sup> to 5 × 10<sup>7</sup> J/mol-VOC in the surface discharge plasma [15,20]. The required energy for AcH decomposition may be less. The potential decomposition rate for AcH by plasma is larger than 20 μmol/min at the input power of 5 W. From these values, the contribution of photocatalysis induced by UV light of the plasma is estimated to be less than 0.2% against the AcH decomposition by the plasma. Since this contribution was obtained by assuming the quantum efficiency of photocatalytic reaction is 100%, the only way to increase the contribution is to increase the UV emission efficiency from plasma dramatically.

### 3.2. Effects of catalysts existing in plasma

The effects of catalysts, ultrafine TiO<sub>2</sub> and γ-Al<sub>2</sub>O<sub>3</sub>, in non-thermal plasma on oxidation reaction were investigated. As a model reaction, the oxidation of CO into CO<sub>2</sub> by surface discharge plasma was analyzed. Effects of deposition of Pt on TiO<sub>2</sub> and Al<sub>2</sub>O<sub>3</sub> were also analyzed since Pt deposited on TiO<sub>2</sub> enhances the photocatalytic oxidation of CO [24,25]. The reaction atmosphere was Ar/O<sub>2</sub> mixture (50%) containing trace amount of N<sub>2</sub> as illuminant, because plasma in the atmospheric air (N<sub>2</sub>/O<sub>2</sub>) produces HNO<sub>3</sub>, which could deactivate the oxidation sites of TiO<sub>2</sub> [26].

When the surface discharge plasma was generated, the concentration of CO decreased and the concentration of CO<sub>2</sub> increased. Since the decrease in CO concentration was nearly same as the increase in CO<sub>2</sub> concentration, it is considered that CO was oxidized into CO<sub>2</sub> as Eq. (3)



The oxidation rate was 29 μmol/h at the input power of 5 W without catalyst, and the CO conversion was 23%. The CO conversion was improved by all of the catalysts analyzed (Fig. 5a). The enhancement effects by the Al<sub>2</sub>O<sub>3</sub> group were larger than

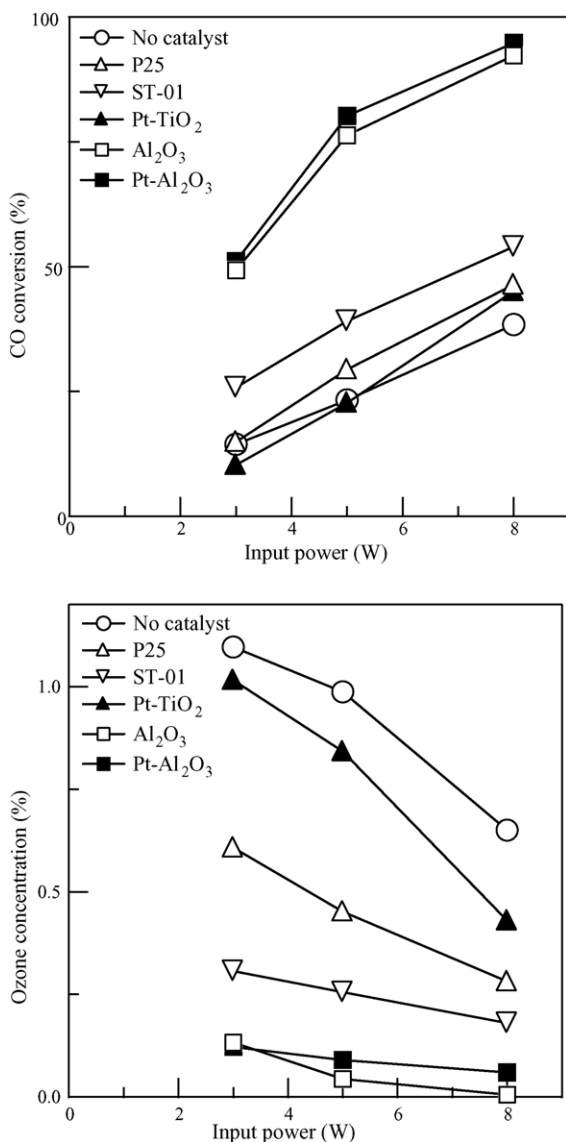


Fig. 5. CO conversions (a) and O<sub>3</sub> concentrations (b) obtained by the plasma enhanced catalytic reactor.

those by the TiO<sub>2</sub> group. Compared with two type of TiO<sub>2</sub>, ST-01 (relative surface area = 300 m<sup>2</sup>/g) showed the higher activity than P25 (50 m<sup>2</sup>/g). This suggests that the surface of catalysts are responsible for the CO oxidation. Also, since the activity of Al<sub>2</sub>O<sub>3</sub> (200 m<sup>2</sup>/g) was higher than that of ST-01, the surface of  $\gamma$ -Al<sub>2</sub>O<sub>3</sub> seems to be effective on the CO oxidation rather than that of TiO<sub>2</sub>. The deposition of Pt on TiO<sub>2</sub> or Al<sub>2</sub>O<sub>3</sub> did not change their activity significantly.

TiO<sub>2</sub> and Al<sub>2</sub>O<sub>3</sub> coated in the barrier tube suppressed the concentration of O<sub>3</sub> (Fig. 5b). This is due to (i) the inhibition of O<sub>3</sub> production or (ii) the decomposition of produced O<sub>3</sub>. Since O<sub>3</sub> was formed in the plasma without surface, the later reason seems important. The suppression effects of Al<sub>2</sub>O<sub>3</sub> group were stronger than those of TiO<sub>2</sub> group. Approximately, the catalyst with stronger O<sub>3</sub>-suppression effect showed the higher CO-oxidation activity. The relation between O<sub>3</sub> decomposition and the CO oxidation is discussed later.

In the photocatalytic oxidation of CO, the deposition of Pt particles on TiO<sub>2</sub> increased the CO oxidation rate. It was explained that Pt on TiO<sub>2</sub> acted as the active sites on which CO was chemically adsorbed and was oxidized to CO<sub>2</sub> [25]. In the present paper, the deposition of Pt on TiO<sub>2</sub> did not increase the CO oxidation rate significantly. Therefore, the enhancement of CO oxidation by TiO<sub>2</sub> was not a photocatalytic effect. Also, the increase in the CO oxidation rate by Al<sub>2</sub>O<sub>3</sub> is not due to photocatalytic effect because the UV adsorption of Al<sub>2</sub>O<sub>3</sub> is weak. The conventional catalytic effect of Al<sub>2</sub>O<sub>3</sub> surface or the direct excitation of Al<sub>2</sub>O<sub>3</sub> by plasma may be responsible for the enhancement of CO oxidation.

The roles of catalyst and ozone on CO oxidation were further analyzed with the combined reactor shown in Fig. 1d. The thermal reactor composed of a quartz tube and the catalyst was connected at the downstream of the plasma reactor. No catalyst was contained in the plasma reactor. The reaction gas containing CO was passed through the system, and the temperature of the reactor was controlled by a thermoregulator. When the plasma was not generated, Al<sub>2</sub>O<sub>3</sub> and TiO<sub>2</sub> did not oxidize CO at the temperatures between 40 and 180 °C (Fig. 6a). Only

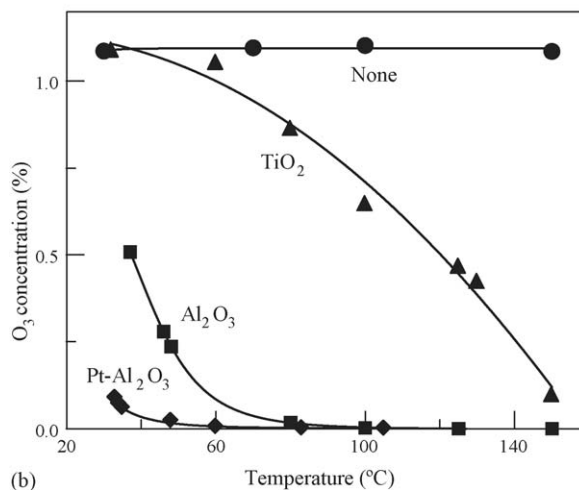
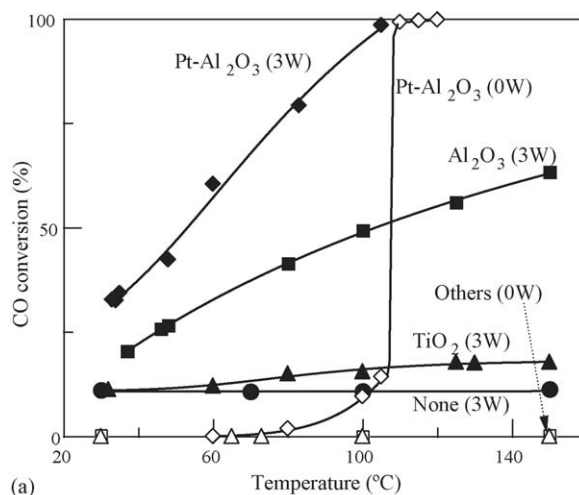


Fig. 6. CO conversions by the combined reactors (a) and O<sub>3</sub> concentrations in the outlet gas (b) plotted against the temperature of catalytic reactor. The plasma reactor was operated at 3 W.

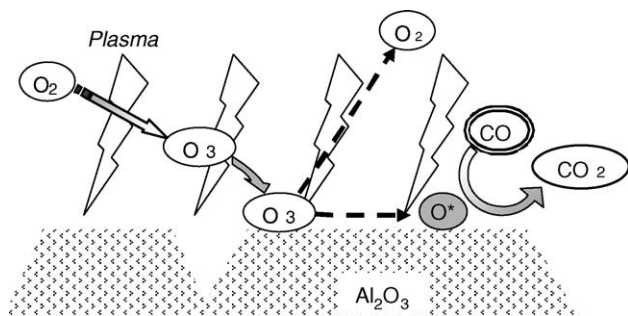


Fig. 7. Proposed mechanism of the CO oxidation in the presence of  $\text{Al}_2\text{O}_3$  and plasma.

$\text{Pt-Al}_2\text{O}_3$  oxidized CO at the temperatures above  $80^\circ\text{C}$ . This can be ascribed to the catalytic oxidation activity of Pt with  $\text{O}_2$ . When the plasma was generated at 3 W and  $\text{O}_3$  was supplied to the catalytic reactor,  $\text{Pt-Al}_2\text{O}_3$  and  $\text{Al}_2\text{O}_3$  oxidized CO even at the room temperature. The oxidation activity of  $\text{TiO}_2$  with  $\text{O}_3$  was smaller, and CO was not oxidized without catalyst. These results suggest that CO was oxidized by active species formed on surface of  $\text{Al}_2\text{O}_3$  by the decomposition of  $\text{O}_3$ . In the experiment using the setup c in Fig. 1, the surface temperature of plasma reactor became  $48\text{--}83^\circ\text{C}$  at the input power of 3–8 W. These temperatures are high enough to take advantage of the catalytic activity of  $\text{Al}_2\text{O}_3$ -based catalyst for CO oxidation.

Fig. 6b shows the  $\text{O}_3$  concentration in the effluent from the combined reactor at the input power of 3 W. Without catalyst, the  $\text{O}_3$  concentration became ca. 1%. This high concentration is due to the high percentage of  $\text{O}_2$  in the reaction atmosphere ( $\text{Ar}/\text{O}_2 = 50/50$ ). The  $\text{O}_3$  concentration was decreased by the catalytic reactor with  $\text{Al}_2\text{O}_3$ ,  $\text{Pt-Al}_2\text{O}_3$ , and  $\text{TiO}_2$ , and was suppressed effectively at higher temperatures. This indicates that catalytic decomposition of  $\text{O}_3$  into  $\text{O}_2$  took place. The  $\text{O}_3$  decomposition activity was stronger in the order of  $\text{Pt-Al}_2\text{O}_3 > \text{Al}_2\text{O}_3 > \text{TiO}_2$ . The catalyst with high  $\text{O}_3$  decomposition activity coincided with the catalyst with high CO oxidation activity. The  $\text{O}_3$  decomposition on the catalyst was accompanied by formations of active species ( $\text{O}^*$  and  $\text{O}_2^*$ ) [27]. Therefore, it is considered that the active species formed by the  $\text{O}_3$  decomposition oxidized CO into  $\text{CO}_2$  as shown in Fig. 7.

The possibility of direct activation of catalyst by plasma was evaluated. The surface temperature of plasma reactor was  $48^\circ\text{C}$  at the input power of 3 W. In the presence of plasma (Fig. 1c), the difference between the CO conversions with  $\text{Al}_2\text{O}_3$  and without catalyst was 35% at 3 W (Fig. 5a). In the absence of plasma (Fig. 1d), the difference was only 15% at  $50^\circ\text{C}$  in the presence of  $\text{O}_3$  (Fig. 6a). Thus, the CO conversion by  $\text{Al}_2\text{O}_3$  in the plasma was significantly larger than that without plasma, assuming that the temperature of  $\text{Al}_2\text{O}_3$  in the plasma was similar to the temperature of reactor surface. This suggests that the catalyst existing in plasma has some effects other than the conventional thermal catalysis, such as direct activation of the catalyst by plasma discharge. It was reported that the surface oxygen (or lattice oxygen) of  $\text{TiO}_2$  or  $\alpha\text{-Al}_2\text{O}_3$  is activated by the effect of

plasma discharge and is released from the solid phase [21]. If the activity of surface oxygen of  $\gamma\text{-Al}_2\text{O}_3$  is also increased by plasma, the oxidation of CO and the decomposition of  $\text{O}_3$  are possibly enhanced by the activated surface oxygen. To clarify the behavior of the surface oxygen in plasma, the precise analysis of temperature and isotope techniques are effective.

#### 4. Conclusion

- The contribution of photocatalysis induced by UV light from the surface discharge plasma on the AcH decomposition by the plasma is estimated to be less than 0.2%.
- The coating of  $\gamma\text{-Al}_2\text{O}_3$  on the inside wall of plasma reactor improved the oxidation rate dramatically. The high activity of  $\text{Al}_2\text{O}_3$  is due to the catalytic activity that utilizes  $\text{O}_3$  and heat. The direct activation of the surface oxygen by plasma was also suggested.
- To improve energy efficiency of the VOCs decomposition by plasma method, improvements of catalysts that utilize  $\text{O}_3$  and lattice oxygen are more important than improvements of photocatalyst activated by weak UV light derived from the plasma.

#### References

- [1] A.P. Jones, *Atmos. Environ.* 33 (1999) 4535.
- [2] P. Wargocki, Z. Bako-Biro, G. Clausen, P.O. Fanger, *Energy Build.* 34 (2002) 775.
- [3] P. Wolkoff, G.D. Nielsen, *Atmos. Environ.* 35 (2001) 4407.
- [4] P.O. Fanger, *Int. J. Refrigerat.* 24 (2001) 148.
- [5] E. Racciatti, J. Vecchiet, A. Ceccomancini, F. Ricci, E. Pizzigallo, *Sci. Total Environ.* 270 (2001) 27.
- [6] S. Futamura, A. Zhang, H. Einaga, H. Kabashima, *Catal. Today* 72 (2002) 259.
- [7] D. Evans, L.A. Rosocha, G.K. Anderson, J.J. Coogan, M.J. Kushner, *J. Appl. Phys.* 74 (1993) 5378.
- [8] M.R. Hoffmann, S.T. Martin, W. Choi, D.W. Bahnemann, *Chem. Rev.* 95 (1995) 69.
- [9] M.D. Driessen, A.L. Goodman, T.M. Miller, G.A. Zaharias, V.H. Grassian, *J. Phys. Chem. B* 102 (1998) 549.
- [10] K.I. Zamaraev, M.I. Khramov, V.N. Parmon, *Catal. Rev.* 35 (1994) 617.
- [11] T. Sano, N. Negishi, S. Kutsuna, K. Takeuchi, *J. Mol. Catal. A: Chem.* 168 (2001) 233.
- [12] H. Einaga, S. Futamura, T. Ibusuki, *Phys. Chem. Chem. Phys.* 1 (1999) 4903.
- [13] E. Obushi, T. Sakamoto, K. Nakano, F. Shiraiishi, *Chem. Eng. Sci.* 54 (1999) 1525.
- [14] J.L. Falconer, K.A. Magrini-Bair, *J. Catal.* 179 (1998) 171.
- [15] H.H. Kim, *Plasma Process. Polym.* 1 (2004) 91.
- [16] J. Arno, J.W. Bevan, M. Moisan, *Environ. Sci. Technol.* 30 (1996) 2427.
- [17] A. Dono, C. Paradisi, G. Scorrano, *Rapid Comm. Mass Spectrometry* 11 (1997) 1687.
- [18] B.Y. Lee, S.H. Park, S.C. Lee, M. Kang, S.J. Choung, *Catal. Today* 93/95 (2004) 769.
- [19] D. Li, D. Yakushiji, S. Kanazawa, T. Ohkubo, Y. Nomoto, *J. Electrostat.* 55 (2002) 311.
- [20] H.H. Kim, Y.H. Lee, A. Ogata, S. Futamura, *Catal. Comm.* 4 (2003) 347.
- [21] A. Ogata, H.H. Kim, S. Futamura, S. Kushiya, K. Mizuno, *Appl. Catal. B: Environ.* 53 (2004) 175.
- [22] S. Futamura, H. Einaga, H. Kabashima, L.Y. Hwan, *Catal. Today* 89 (2004) 89.

- [23] T. Sano, N. Negishi, K. Uchino, J. Tanaka, S. Matsuzawa, K. Takeuchi, J. Photochem. Photobiol. A: Chem. 160 (2003) 93.
- [24] A.V. Vorontsova, E.N. Savinova, J. Zhensheng, J. Photochem. Photobiol. A: Chem. 125 (1999) 113.
- [25] H. Einaga, M. Harada, S. Futamura, T. Ibusuki, J. Phys. Chem. B 107 (2003) 9290.
- [26] T. Ibusuki, K. Takeuchi, Atmos. Environ. 20 (1986) 1711.
- [27] W. Li, G.V. Gibbs, S.T. Oyama, J. Am. Chem. Soc. 120 (1998) 9041.